

Supporting Information

A spin-1/2 gapped compound CdCu₂(SeO₃)₂Cl₂ with a ladder structure

Mengsi Zhang,^{a,b} Meiyuan Cui,^a Zhiying Zhao,^a Xing Huang,^a and Zhangzhen He*,^a

^aState Key Laboratory of Structural Chemistry, Fujian Institute of Research on the Structure of Matter, Chinese Academy of Sciences, Fuzhou, Fujian 350002, P. R. China

^bUniversity of Chinese Academy of Sciences, Beijing 100049, P. R. China

*E-mail: hczi988@hotmail.com, hezz@fjirsm.ac.cn

Fig. S1. The single crystal of $\text{CdCu}_2(\text{SeO}_3)_2\text{Cl}_2$.

Fig. S2. Refinement of powder X-ray ($\text{Cu K}\alpha$) diffraction patterns for $\text{CdCu}_2(\text{SeO}_3)_2\text{Cl}_2$

Fig. S3. The energy-dispersive spectrometry (EDS) elemental analyses of $\text{CdCu}_2(\text{SeO}_3)_2\text{Cl}_2$.

Fig. S4. The spin-ladders of $\text{CdCu}_2(\text{SeO}_3)_2\text{Cl}_2$ connected by SeO_3^{2-} groups in the bc plane.

Fig. S5. The chains of (a) $\text{SrCu}_2(\text{SeO}_3)_2\text{Cl}_2$ and $\text{PbCu}_2(\text{SeO}_3)_2\text{Cl}_2$.

Fig. S6. Views of the coordination geometry for (a) Cd atom in $\text{CdCu}_2(\text{SeO}_3)_2\text{Cl}_2$, (b) Sr atom in $\text{SrCu}_2(\text{SeO}_3)_2\text{Cl}_2$ and (c) Pb atom in $\text{PbCu}_2(\text{SeO}_3)_2\text{Cl}_2$.

Fig. S7. Specific heat ($C/T-T$) of $\text{CdCu}_2(\text{SeO}_3)_2\text{Cl}_2$ measured at 0 T.

Fig. S8. Magnetic susceptibilities using single sample measured along different directions.

Fig. S9. Magnetic susceptibility of $\text{CdCu}_2(\text{SeO}_3)_2\text{Cl}_2$ for polycrystalline sample at 0.5 T. The green line is a fit using the mean-field Bleaney-Bowers expression.

Fig. S10. Magnetic susceptibility of $\text{CdCu}_2(\text{SeO}_3)_2\text{Cl}_2$ for polycrystalline sample at 0.5 T. The pink line is a fit using the Hatfield's chain model.

Fig. S11. IR spectra of $\text{CdCu}_2(\text{SeO}_3)_2\text{Cl}_2$.

Fig. S12. UV-vis-NIR spectra of $\text{CdCu}_2(\text{SeO}_3)_2\text{Cl}_2$.

Fig. S13. The TGA curve for $\text{CdCu}_2(\text{SeO}_3)_2\text{Cl}_2$.

Table S1. Crystal data and structure refinements for $\text{CdCu}_2(\text{SeO}_3)_2\text{Cl}_2$.

Table S2. Atomic coordinates and equivalent isotropic displacement parameters for $\text{CdCu}_2(\text{SeO}_3)_2\text{Cl}_2$.

Table S3. Anisotropic displacement parameters for $\text{CdCu}_2(\text{SeO}_3)_2\text{Cl}_2$.

Table S4. Bond lengths [\AA] and angles [deg] for $\text{CdCu}_2(\text{SeO}_3)_2\text{Cl}_2$.

Experimental details:

1. Synthesis. CdCu₂(SeO₃)₂Cl₂ was synthesized by hydrothermal reaction. The mixture of 1 mmol CdCl₂ (AR, 0.1833 g), 2 mmol CuO (AR, 0.1591 g), 2 mmol SeO₂ (AR, 0.2219 g), and 2 mL deionized water was loaded into a 28 mL Teflon-lined autoclave. The autoclaves were heated at 230 °C for 3 days under autogenous pressure, and cooled to 35 °C for 5 days. The green and block crystals were obtained (Fig. S1). The purity of powdered samples was examined by powder X-ray diffraction analysis (Fig. S2), and Rietveld refinement for structural parameters was carried out by GSAS-EXPGUI.¹ The EDS (Fig. S3) analyses gave average molar ratios of 1.0/2.1/1.9 for Cd/Se/Cu, which is in accordance with the stoichiometric ratio of CdCu₂(SeO₃)₂Cl₂. The calculated bond valences of Cd, Cu, and Se atoms are 1.91, 2.07, and 3.98, respectively. The valence state of Cd, Cu, and Se atoms was proved to be +2, +2, and +4, respectively.

2. X-ray crystallographic studies. The single crystal X-ray diffraction data (XRD) for CdCu₂(SeO₃)₂Cl₂ were recorded on Rigaku Mercury CCD diffractometer equipped with a graphite-monochromated Mo-K α radiation at 293 K. The structure was solved by direct methods and refined by full-matrix least-squares fitting on F^2 using Olex2.² The final refined structural parameters were verified by the PLATON program.³ Crystallographic data are summarized in Table S1, and the detailed bond lengths and angles are shown in Table S2-4. The orientation of single crystals was determined using an Agilent Technologies SuperNova CCD diffractometer.

3. Magnetic Measurements. Magnetic and specific heat measurements were carried

out on Quantum Design Physical Property Measurement System (PPMS). Magnetic susceptibilities of $\text{CdCu}_2(\text{SeO}_3)_2\text{Cl}_2$ for powdered and single-crystal samples were measured between 2 and 300 K at 0.5 T. The single-crystal sample was measured with an applied field parallel and perpendicular to the *c*-axis. The isothermal magnetization was measured at 2 K. The measurement of specific heat was under zero field. The measured data were corrected by background correction for sample holders and Pascal constants.⁴

4. Optical Measurements. Infrared (IR) spectra were performed on the Magna 750 FT-IR spectrometer with KBr pellets from 400 to 4000 cm^{-1} . Ultraviolet–visible–near infrared (UV–vis–NIR) spectra from 200 to 2000 nm were measured on a PerkinElmer Lambda 950 UV–vis–NIR spectrophotometer.

The IR spectrum (Fig. S10) exhibits that the absorption peaks at 514, 543, 650, 775 and 843 cm^{-1} can be assigned to the characteristic peaks of SeO_3^{2-} groups.^{5,6} UV–vis–NIR spectra (Fig. S11) present a broad and strong absorption peak at the range of 1200–600 nm corresponding to ${}^2\text{T}_{2g}\rightarrow{}^2\text{E}_g$ transition. Besides, the slightly fissurate peak may be on account of different bond lengths of distorted CuO_4Cl_2 octahedra in the crystal field.⁷ Also, the spectra (the inset of Fig. S11) reveal the band gap of 2.95 eV, suggesting $\text{CdCu}_2(\text{SeO}_3)_2\text{Cl}_2$ is wide band gap semiconductor.

5. Thermal Analysis. Thermogravimetric analysis (TGA) of $\text{CdCu}_2(\text{SeO}_3)_2\text{Cl}_2$ was performed on the NETZSCH STA 449F3 instrument under a N_2 flow at a heating speed of 15 °C/min from room temperature to 1000 °C.

Thermal analysis (Fig. S12) indicates that $\text{CdCu}_2(\text{SeO}_3)_2\text{Cl}_2$ is stable below

450 °C. The first step occurs in the temperature range of 450 °C to 640 °C, corresponding to the release of two SeO₂ molecules. The observed weight loss 38.2% is in good agreement with the theoretical value of 39.4%. Further heating, the second weight loss of 32.3% from 640 to 935 °C is attributed to the loss of one CdCl₂ molecule, which is close to the calculated value of 33.2%. Similar decomposition can be found in Cd₅(SeO₃)₄Cl₂(H₂O).⁸ Finally, the process of weight reduction was finished around 935 °C. While the final residuals are not further characterized owing to the fact that the residuals were melted with the TGA bucket made of Al₂O₃ under very high temperature.

References:

- 1 B. H. Toby, *J. Appl. Crystallogr.*, 2001, **34**, 210.
- 2 O. V. Dolomanov, L. J. Bourhis, R. J. Gildea, J. A. K. Howard, and H. Puschmann, *J. Appl. Cryst.*, 2009, **42**, 339–341.
- 3 A. L. Spek, *Acta Crystallogr., Sect. D: Biol. Crystallogr.*, 2009, **65**, 148–155.
- 4 G. A. Bain, and J. F. Berry, *J. Chem. Educ.*, 2008, **85**, 532–536.
- 5 Y. P. Gong, C. L. Hu, Y. X. Ma, J. G. Mao, and F. Kong, *Inorg. Chem. Front.*, 2019, **6**, 3133–3139.
- 6 F. Kong, Q. P. Lin, F. Y. Yi, and J. G. Mao, *Inorg. Chem.*, 2009, **48**, 6794–6803.
- 7 L. Geng, H. Wang, Q. Li, H. Y. Lu, and G. Li, *Dalton Trans.*, 2018, **47**, 13466–13471.
- 8 M. Shang, L. Liu, and P. S. Halasyamani, *J. Solid State Chem.*, 2019, **273**, 106–111.



Fig. S1. The single crystal of $\text{CdCu}_2(\text{SeO}_3)_2\text{Cl}_2$.

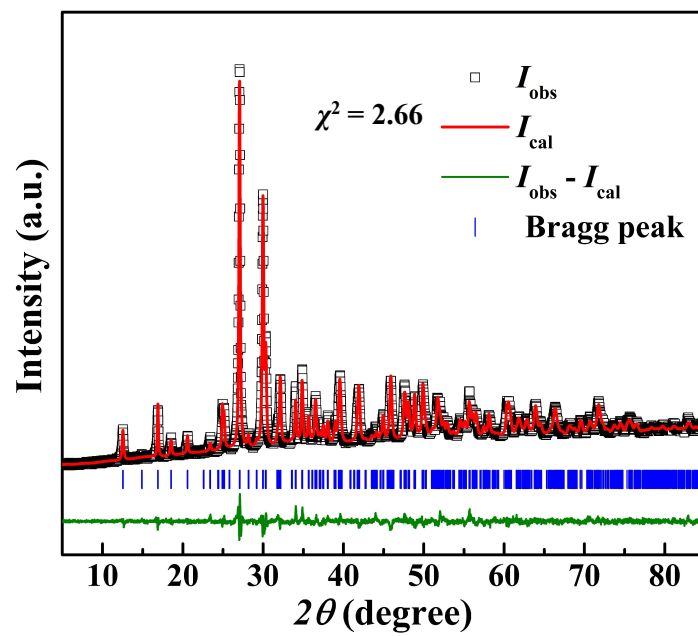


Fig. S2. Refinement of powder X-ray (Cu K α) diffraction patterns for $\text{CdCu}_2(\text{SeO}_3)_2\text{Cl}_2$.

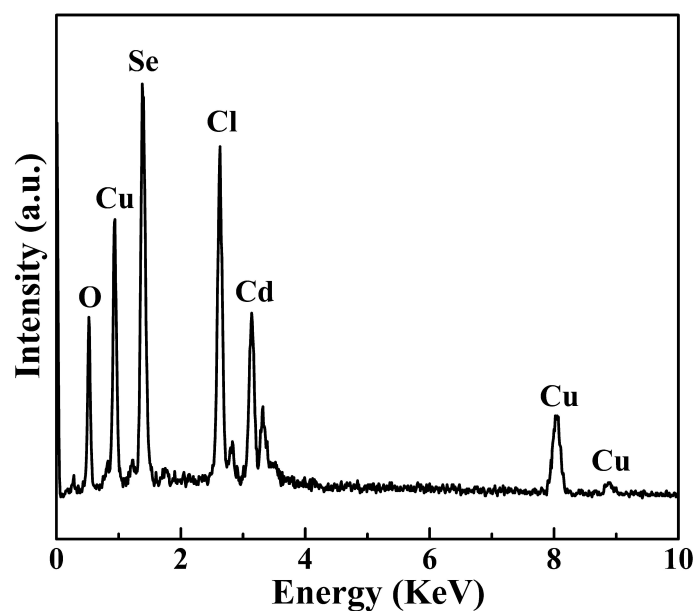


Fig. S3. The energy-dispersive spectrometry (EDS) elemental analyses of $\text{CdCu}_2(\text{SeO}_3)_2\text{Cl}_2$.

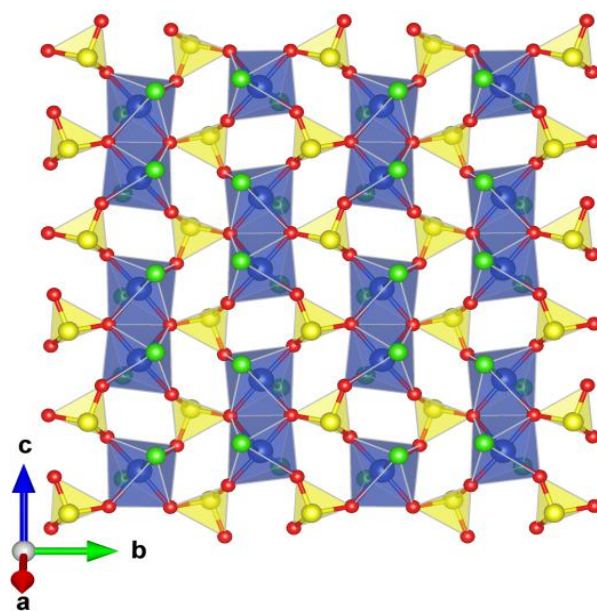


Fig. S4. The spin-ladders of $\text{CdCu}_2(\text{SeO}_3)_2\text{Cl}_2$ connected by SeO_3^{2-} groups in the bc plane.

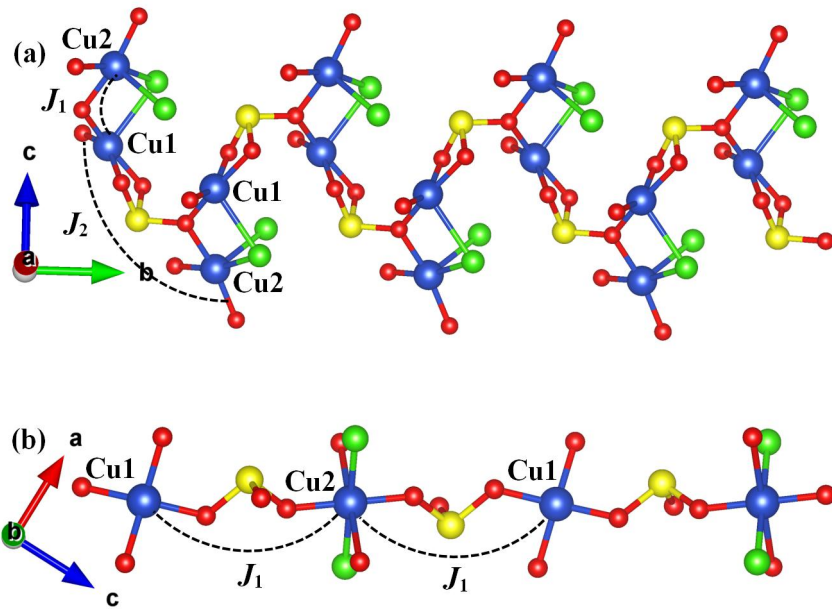


Fig. S5. The Cu-chains of (a) $\text{SrCu}_2(\text{SeO}_3)_2\text{Cl}_2$ and $\text{PbCu}_2(\text{SeO}_3)_2\text{Cl}_2$.

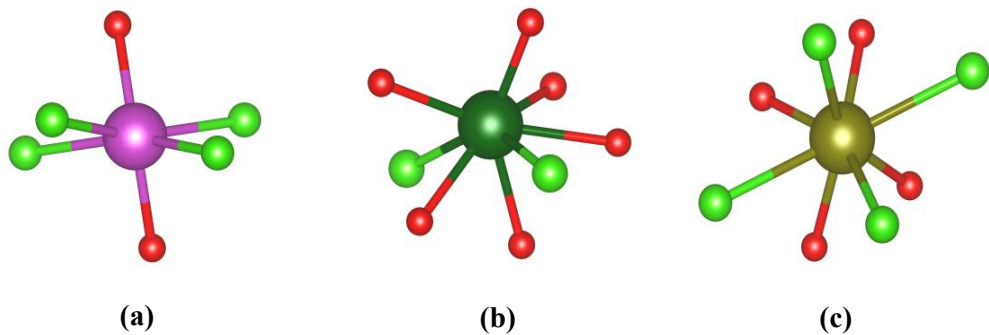


Fig. S6. Views of the coordination geometry for (a) Cd atom in $\text{CdCu}_2(\text{SeO}_3)_2\text{Cl}_2$, (b) Sr atom in $\text{SrCu}_2(\text{SeO}_3)_2\text{Cl}_2$ and (c) Pb atom in $\text{PbCu}_2(\text{SeO}_3)_2\text{Cl}_2$.

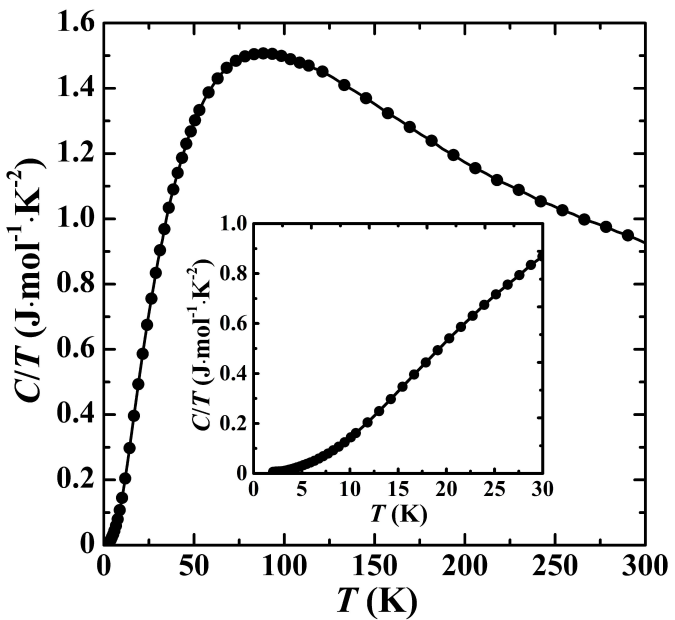


Fig. S7. Specific heat ($C/T-T$) of $\text{CdCu}_2(\text{SeO}_3)_2\text{Cl}_2$ measured at 0 T.

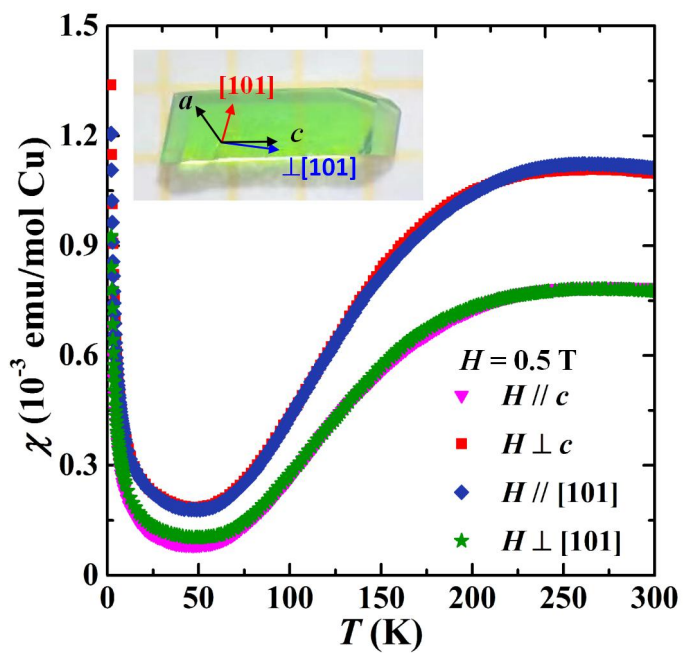


Fig. S8. Magnetic susceptibilities using single sample measured along different directions.

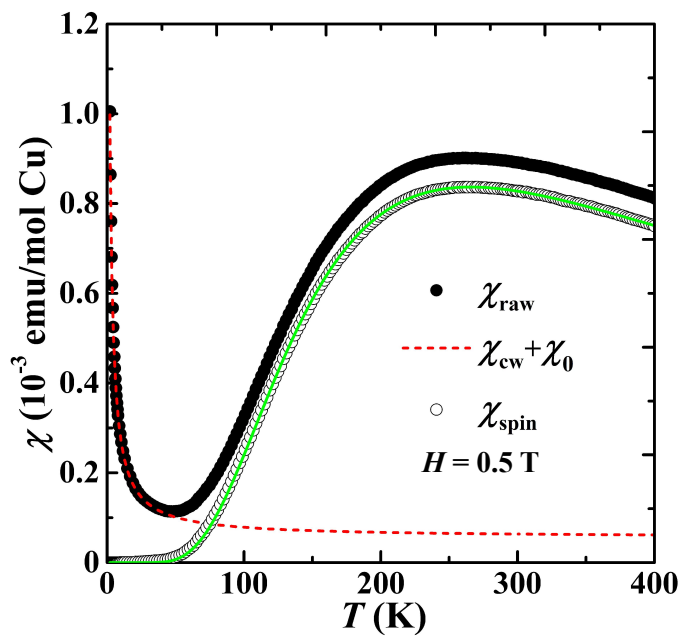


Fig. S9. Magnetic susceptibility of $\text{CdCu}_2(\text{SeO}_3)_2\text{Cl}_2$ for polycrystalline sample at 0.5 T. The green line is a fit using the mean-field Bleaney-Bowers expression.

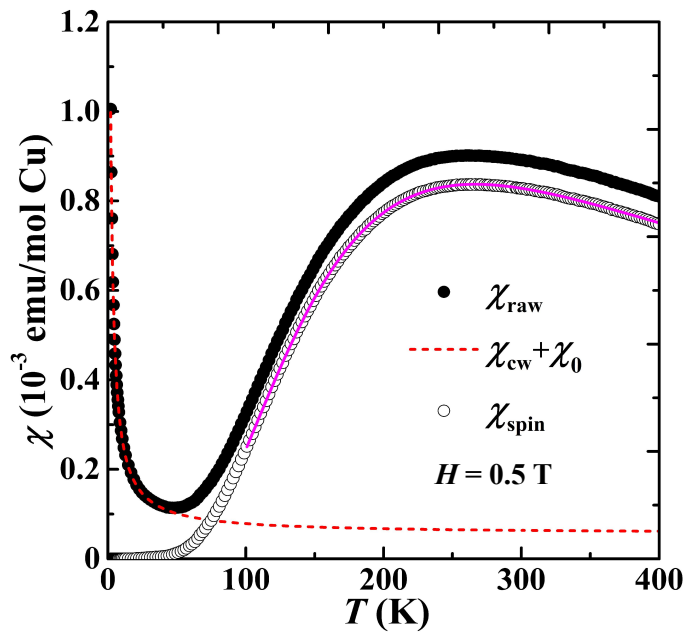


Fig. S10. Magnetic susceptibility of $\text{CdCu}_2(\text{SeO}_3)_2\text{Cl}_2$ for polycrystalline sample at 0.5 T. The pink line is a fit using the Hatfield's chain model.

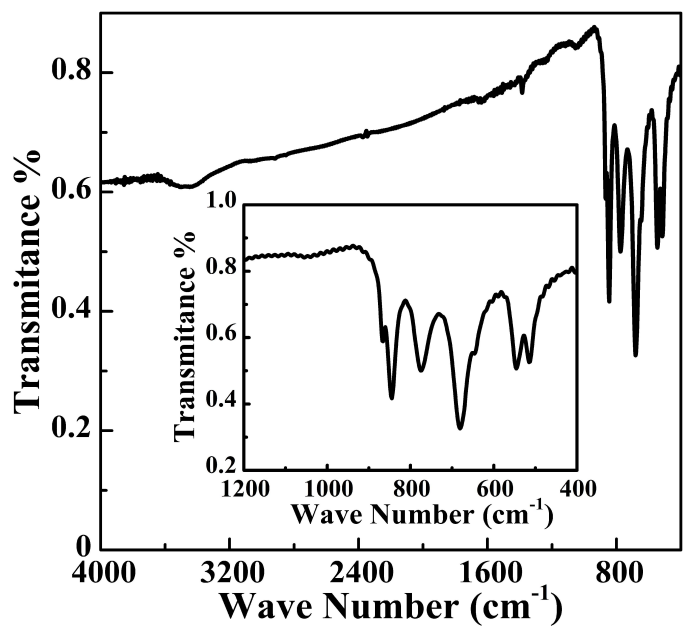


Fig. S11. IR spectra of $\text{CdCu}_2(\text{SeO}_3)_2\text{Cl}_2$.

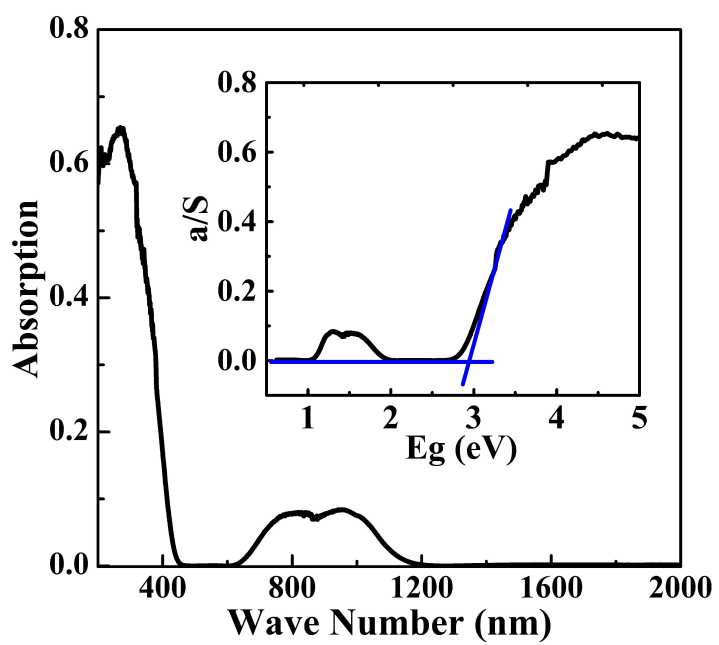


Fig. S12. UV-vis-NIR spectra of $\text{CdCu}_2(\text{SeO}_3)_2\text{Cl}_2$.

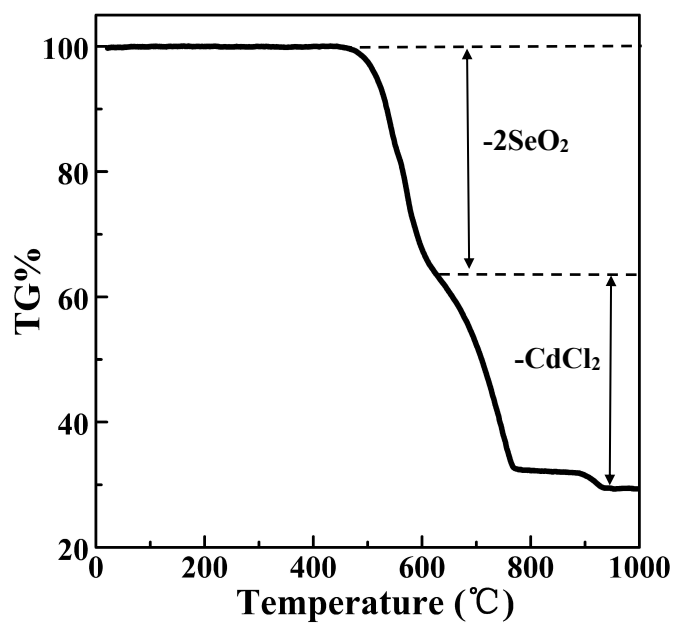


Fig. S13. The TGA curve for $\text{CdCu}_2(\text{SeO}_3)_2\text{Cl}_2$.

Table S1. Crystal data and structure refinements for CdCu₂(SeO₃)₂Cl₂.

compound	CdCu ₂ (SeO ₃) ₂ Cl ₂
formula weight	564.33
T, K	room temperature
λ, Å	0.71073
space group	C2/c
a, Å	11.9190(5)
b, Å	9.6321(3)
c, Å	7.8264(2)
β, deg	117.547(3)
V, Å ³	796.65(5)
Z	4
D _{calcd} , g cm ⁻³	4.705
μ, mm ⁻¹	17.730
GOF on F ²	1.179
R ₁ , wR ₂ [I > 2σ(I)] ^a	0.0191, 0.0476
R ₁ , wR ₂ (all data)	0.0205, 0.0481

^aR₁ = $\frac{\sum ||F_o| - |F_c||}{\sum |F_o|}$, and wR₂ = $\left\{ \frac{\sum w[(F_o)^2 - (F_c)^2]^2}{\sum w[(F_o)^2]^2} \right\}^{1/2}$.

Table S2. Atomic coordinates ($\times 10^4$) and equivalent isotropic displacement parameters ($\text{\AA}^2 \times 10^3$) for $\text{CdCu}_2(\text{SeO}_3)_2\text{Cl}_2$. U_{eq} is defined as one third of the trace of the orthogonalized U_{ij} tensor.

Atom	x	y	z	$U(\text{eq})$
Cd(1)	0	-320(1)	2500	13(1)
Se(1)	-3371(1)	-394(1)	-290(1)	7(1)
Cu(1)	-2776(1)	2513(1)	1757(1)	9(1)
Cl(1)	305(1)	1767(1)	565(1)	14(1)
O(1)	-2723(2)	1240(2)	-184(3)	12(1)
O(2)	-2056(2)	-1160(2)	1501(3)	11(1)
O(3)	-3439(2)	-984(2)	-2341(3)	13(1)

Table S3. Anisotropic displacement parameters ($\text{\AA}^2 \times 10^3$) for $\text{CdCu}_2(\text{SeO}_3)_2\text{Cl}_2$. The anisotropic displacement factor exponent takes the form:

$$-2\pi^2[h^2a^*{}^2U_{11} + 2hka^*b^*U_{12} + \dots].$$

Atom	U_{11}	U_{22}	U_{33}	U_{23}	U_{13}	U_{12}
Cd(1)	15(1)	15(1)	12(1)	0	8(1)	0
Se(1)	9(1)	6(1)	6(1)	0(1)	4(1)	-1(1)
Cu(1)	17(1)	6(1)	8(1)	-1(1)	9(1)	-1(1)
Cl(1)	14(1)	15(1)	12(1)	0(1)	6(1)	-2(1)
O(1)	21(1)	9(1)	11(1)	-2(1)	11(1)	-4(1)
O(2)	13(1)	10(1)	10(1)	4(1)	5(1)	2(1)
O(3)	23(1)	10(1)	7(1)	-2(1)	7(1)	2(1)

Table S4. Bond lengths [Å] and angles [deg] for CdCu₂(SeO₃)₂Cl₂.

Cd(1)-Cl(1)#1	2.6497(8)	O(2)#2-Cd(1)-Cl(1)#3	78.77(6)
Cd(1)-Cl(1)#2	2.6416(8)	O(2)#2-Cd(1)-Cl(1)#2	118.11(6)
Cd(1)-Cl(1)	2.6415(8)	O(2)#2-Cd(1)-Cl(1)	93.11(6)
Cd(1)-Cl(1)#3	2.6497(8)	O(2)-Cd(1)-Cl(1)#1	78.77(6)
Cd(1)-O(2)#2	2.344(2)	O(2)#2-Cd(1)-Cl(1)#1	80.31(6)
Cd(1)-O(2)	2.344(2)	O(2)-Cd(1)-O(2)#2	139.62(11)
Se(1)-O(1)	1.739(2)	O(2)-Se(1)-O(1)	97.63(11)
Se(1)-O(2)	1.713(2)	O(3)-Se(1)-O(1)	100.17(11)
Se(1)-O(3)	1.669(2)	O(3)-Se(1)-O(2)	105.04(11)
Cu(1)-Cl(1)#2	2.8065(9)	Cl(1)#5-Cu(1)-Cl(1)#2	173.49(4)
Cu(1)-Cl(1)#5	2.7928(9)	O(1)#5-Cu(1)-Cl(1)#2	96.03(8)
Cu(1)-O(1)	1.975(2)	O(1)-Cu(1)-Cl(1)#5	93.59(8)
Cu(1)-O(1)#5	1.997(2)	O(1)-Cu(1)-Cl(1)#2	91.13(8)
Cu(1)-O(2)#4	1.946(2)	O(1)#5-Cu(1)-Cl(1)#5	89.40(8)
Cu(1)-O(3)#1	1.951(2)	O(1)-Cu(1)-O(1)#5	76.97(10)
Cl(1)#2-Cd(1)-Cl(1)#3	157.18(3)	O(2)#4-Cu(1)-Cl(1)#5	82.12(7)
Cl(1)#3-Cd(1)-Cl(1)#1	116.52(4)	O(2)#4-Cu(1)-Cl(1)#2	93.28(7)
Cl(1)#2-Cd(1)-Cl(1)#1	83.05(3)	O(2)#4-Cu(1)-O(1)	175.38(10)
Cl(1)-Cd(1)-Cl(1)#3	83.05(3)	O(2)#4-Cu(1)-O(1)#5	101.16(10)
Cl(1)-Cd(1)-Cl(1)#2	80.88(4)	O(2)#4-Cu(1)-O(3)#1	92.99(10)
Cl(1)-Cd(1)-Cl(1)#1	157.18(3)	O(3)#1-Cu(1)-Cl(1)#5	85.82(8)
O(2)-Cd(1)-Cl(1)#3	80.31(6)	O(3)#1-Cu(1)-Cl(1)#2	89.84(8)
O(2)-Cd(1)-Cl(1)	118.11(6)	O(3)#1-Cu(1)-O(1)#5	164.31(9)
O(2)-Cd(1)-Cl(1)#2	93.11(6)	O(3)#1-Cu(1)-O(1)	88.41(9)

Symmetry transformations used to generate equivalent atoms: #1 x,-y,z+1/2; #2 -x,y,-z+1/2; #3 -x,-y,-z; #4 -x-1/2,y+1/2,-z+1/2; #5 -x-1/2,-y+1/2,-z.